A DNS study of DBD plasma actuators to generate a spatially oscillated spanwise body force to reduce the drag in channel flow

Atilla Altıntaş[†], Lars Davidson and Shia-Hui Peng
Division of Fluid Dynamics, Department of Applied Mechanics, Chalmers University of Technology
SE-412 96 Gothenburg, Sweden
altintas@chalmers.se[†] · lada@chalmers.se · peng@chalmers.se

Abstract

Dielectric Barrier Discharge (DBD) plasma actuators are come forward with their light structures in flow control studies. In spite of the many succesful application of the plasma actuators aligned in flow direction, the drag reduction by spanwise aligned actuation is still need to be addressed. Beside this, recent studies proves that the near wall turbulence structures are modified by the log-law large-scale structures. Therefore a light-structure control device is essential in turbulent boundary layer (TBL) control applications, such as in aircrafts. In this study we investigate the drag reduction cababilities of the DBD plasma actuators in (TBL). First, velocities created by a single DBD plasma actuators are compared with the experiments. After this, a DNS study is performed to obtain a drag reduction by spanwise oscillated DBD plasma force. A drag reduction is achieved in a frictional Reynolds number of $Re_\tau = 180$.

1. Introduction

It is shown that the spanwise oscillated body force is one of the most effective method among the control strategies in TBL. There are a number of methods that creates spatially oscillated spanwise force [3, 5, 7, 8]. For instance electromagnetohydrodynamic (EMHD) control is applied as a spatially oscillated spanwise body force which uses magnets and electrodes to generate the Lorentz force [3]. Although this method provides a large drag reduction, overweight issues makes this method impossible to apply to air vehicles. Recently plasma actuators have become important with their very light forms to control the turbulent boundary layers.

Additionally, there are recent studies which show the high impact of the outer log-low structures in near wall turbulence [1, 2]. Studies also show that increasing the Reynolds number we have higher energy containing structures in the log-low that have higher impact at the wall turbulence.
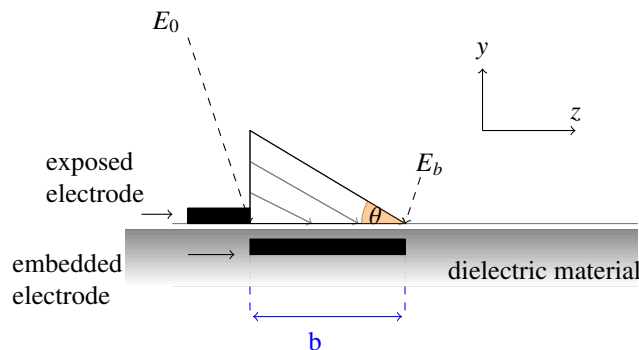

Figure 1: Shyy model illustration. Electric field strength, $E(y, z)$.

Therefore it would be an important achievement to obtain drag reduction with plasma actuators which act as spatially varying spanwise body force. With their light structures plasma actuators could be one of the best candidate to apply to aircrafts to obtain drag reduction. In this study we used Shyy model to mimic the DBD plasma actuators [11].

Shyy model to create the electric field vector generated by a DBD plasma actuator is given as:

$$E(y, z) = E_0 - \frac{E_0 - E_b}{b} z^+ - \frac{E_0 - E_b}{b \tan(\theta)} y^+ \tag{1}$$

Equation 1 is divided into wall-normal and spanwise components, multiplied by Dc.

$$E_z(y, z) = DcE(y, z) \cos \theta, \tag{2}$$

$$E_y(y, z) = DcE(y, z) \sin \theta. \tag{3}$$

Here θ defines the height of the plasma. Dc represents the ratio of the electrical force to the inertial force. E_0 is the maximum electric field strength which decays along the embedded electrode that ceases on the other edge and takes its breakdown strength, E_b. The parameter b is the length of the plasma area, and height of the plasma area is defined by $b \tan(\theta)$.

First we generated an electrical field by a single actuator and we compared the generated velocities with experimental data in stagnant flow [4]. Then we generated a spatially oscillating spanwise body force in stagnant flow by multiple actuators, for continuous and no-spanwise spacing cases. A skin friction reduction of 9% and 4% is obtained, respectively.

2. Direct Numerical Simulations

The governing equations to solve in DNS for an incompressible Newtonian fluid are

$$\frac{\partial \mathbf{u}}{\partial t} + \mathbf{u} \cdot \nabla \mathbf{u} = \hat{\mathbf{e}}_1 \cdot \tilde{\mathbf{I}} - \frac{1}{\rho} \nabla p + \nu \nabla^2 \mathbf{u} + F_z, \tag{4}$$

$$\nabla \cdot \mathbf{u} = 0, \tag{5}$$

where a spanwise directed volume force, F_z, is added as a body force to the Navier-Stokes equations. Here, $\mathbf{u}$, p, ρ, ν are the velocity vector, the pressure, the fluid density, the molecular kinematic viscosity of the fluid, respectively. The first term on the right hand side of Eq. (4) is the driving force in the streamwise direction.

An implicit, two-step time-advancement finite volume methods is used [6]. Central differencing scheme is used in space and the Crank-Nicolson scheme is used in the time domain. The Navier-Stokes equation for u_i, Eq. (4), in discretized from can be written as

$$u_i^{n+1} = u_i^n + \Delta t H\left(u_i^n, u_i^{n+1}\right) - \frac{1}{\rho} \alpha \Delta t \frac{\partial p^{n+1}}{\partial x_i} - \frac{1}{\rho}(1 - \alpha) \Delta t \frac{\partial p^n}{\partial x_i} \tag{6}$$

where $H\left(u_i^n, u_i^{n+1}\right)$ includes convection, the viscous and the source terms, and $\alpha = 0.5$ (Crank-Nicolson). Equation (6) is solved which gives u_i^{n+1} which does not satisfy continuity. An intermediate velocity field is computed by subtracting the implicit part of the pressure gradient, i.e.

$$u_i^* = u_i^{n+1} + \frac{1}{\rho} \alpha \Delta t \frac{\partial p^{n+1}}{\partial x_i}. \tag{7}$$

Taking the divergence of Eq. 7 requiring that continuity (for the face velocities which are obtained by linear interpolation) should be satisfied on level $n + 1$, i.e. $\partial u_{i,f}^{n+1}/\partial x_i = 0$, we obtain

$$\frac{\partial^2 p^{n+1}}{\partial x_i \partial x_i} = \frac{\rho}{\Delta t \alpha} \frac{\partial u_{i,f}^*}{\partial x_i}. \tag{8}$$

The numerical procedure at each time step can be summarized as follows [6].

1. Solve the discretized filtered Navier-Stokes equation for u, v and w.

2. Create an intermediate velocity field u_i^* from Eq. 7.

3. The Poisson equation (Eq. 8) is solved with an efficient multigrid method [?].

4. Compute the face velocities (which satisfy continuity) from the pressure and the intermediate velocity as

$$u_{i,f}^{n+1} = u_{i,f}^* - \frac{1}{\rho} \alpha \Delta t \left(\frac{\partial p^{n+1}}{\partial x_i}\right)_f. \tag{9}$$

5. Step 1 to 4 is performed till convergence (normally two or three iterations) is reached. The convergence for the velocities is 10^{-7} and 10^{-5} for pressure. The residuals are computed using $L1$ norm and they are scaled with the integrated streamwise volume flux (continuity equation) and momentum flux (momentum equations).

6. Next time step.

Note that although no explicit dissipation is introduced to prevent odd-even decoupling, an implicit dissipation is present. The intermediate velocity field is computed at the *cell centres* (see Eq. 7) subtracting a pressure gradient. When, after having solved the pressure Poisson equation, the face velocity field is computed, the pressure gradient at the *faces* (see Eq. 9) is added. This is very similar to the Rhie-Chow dissipation [**? **].

2.1 Validation of the Shyy model

Velocities obtained by numerical model is compared with experiments [4]. A two-dimensional study in a channel is performed. Equations (2) and (3) are solved in two-dimensions (y and z) and the solution is carried out in time until steady state is reached. Slip boundary conditions are applied in the actuator aligned direction (z) and top boundary (high y). The viscosity, $v = 1.81 \times 10^{-5}$ m^2/s, and density, $\rho = 1.25$ kg/m^3. Only the spanwise-directed component of the force is applied ($\theta = 0$), hence only Equation (2) is applied and $E_y = 0$ (i.e. Eq. (3) = 0). The domain size is $125mm \times 100mm$ with grid sizes 98×298 ($y \times z$) for the wall-normal and plasma-aligned directions, respectively. The minimum and maximum grid sizes are $\Delta y_{min} = 0.00025$ m, $\Delta y_{max} = 0.0025$ m with a streching of $y = 1.35$ in the wall normal direction. $\Delta z = 0.00033$ m. The oscillating force is applied in the plasma region ($0.0 < z < 0.02$ m, $0.0 < y < 0.0028$ m). The length of the plasma is $b = 20$ mm. The plasma region is covered by 30×6 cells in the plasma-aligned and wall-normal directions, respectively.

The predicted velocities created by DBD plasma exhibit very similar behaviour compared to the experimental data, see Figs. 2 and 3. The plasma area creates a negative wall-normal velocity upstream of the actuator and a positive wall-normal velocity downstream of the actuator (Figs. 2(a) and 3(a)). The negative area entrains the flow toward wall and the positive area, downstream of the actuator, creates a wall jet which propagates downstream with a velocity parallel to the actuator (Figs. 2(b) and 3(b)). In the experimental study the maximum of the plasma-aligned velocity is 1.8 m/s and the wall-normal velocity is half that, 0.9 m/s. In the numerical study we obtain similar velocity field compared to the experiments (see Fig. 3).
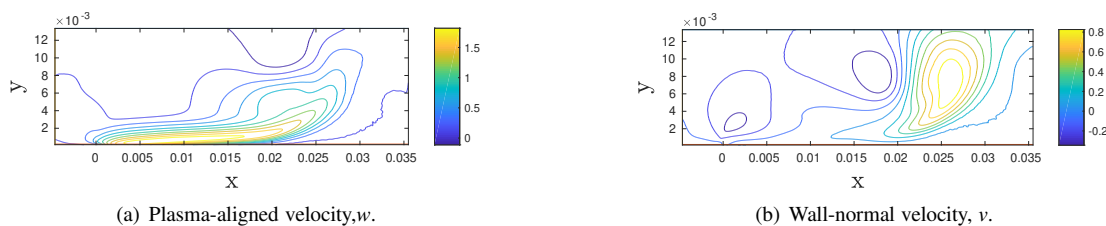

(a) Plasma-aligned velocity, w.

(b) Wall-normal velocity, v.

Figure 2: Plasma-aligned velocity, and wall-normal velocity. [4] Experiments.
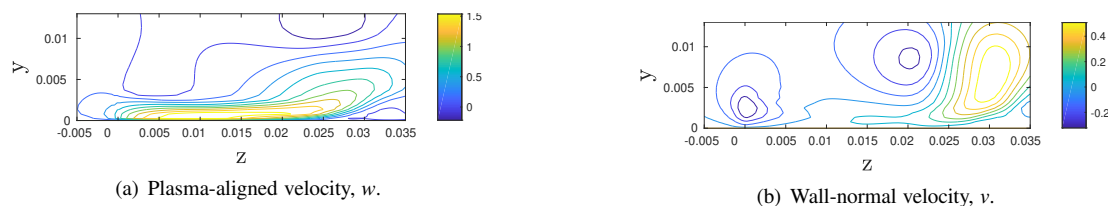

(a) Plasma-aligned velocity, w.

(b) Wall-normal velocity, v.

Figure 3: Plasma-aligned velocity and wall-normal velocity. Numerical study.

3. DBD plasma force

DNS is performed. A spanwise oscillating body force is created by multiple actuators which are aligned in the spanwise direction. Only a spanwise oscillating component of the force is applied ($\theta = 0$ or $F_y = 0$). Equation (2) is modified by applying a sinusoidal variation in the streamwise direction:

$$F_z(y, z) = E(y, z) \, sin(2\pi x^+ / \lambda_x^+). \tag{10}$$

The length of the plasma area, b, is $z^+ = 15$, that defines the maximum width of the plasma in the spanwise direction. The extent of the plasma area in the wall-normal direction is $0 < y^+ < 8$. Two different numerical test cases are studied. A continuous force in the spanwise direction is used in the first case, see Fig. 4(a). In the second test case a discrete force is created by actuators without a space in the spanwise direction, $S_p = 0$, see Fig. 4(b). $Dc = 39.0$ is applied for continuous case and $Dc = 9.0$ is applied for the discrete case. The force oscillates spatially in the streamwise direction and the values range between $\pm 3 \times 10^{-4}$ and $\pm 5.5 \times 10^{-5}$ for the continuous and the discrete cases, respectively. 38 and 19 actuators are used in the spanwise direction for the continuous and the discrete force cases, respectively. The streamwise wavelength of the force for both test cases is $\lambda_x^+ = 180\pi$.
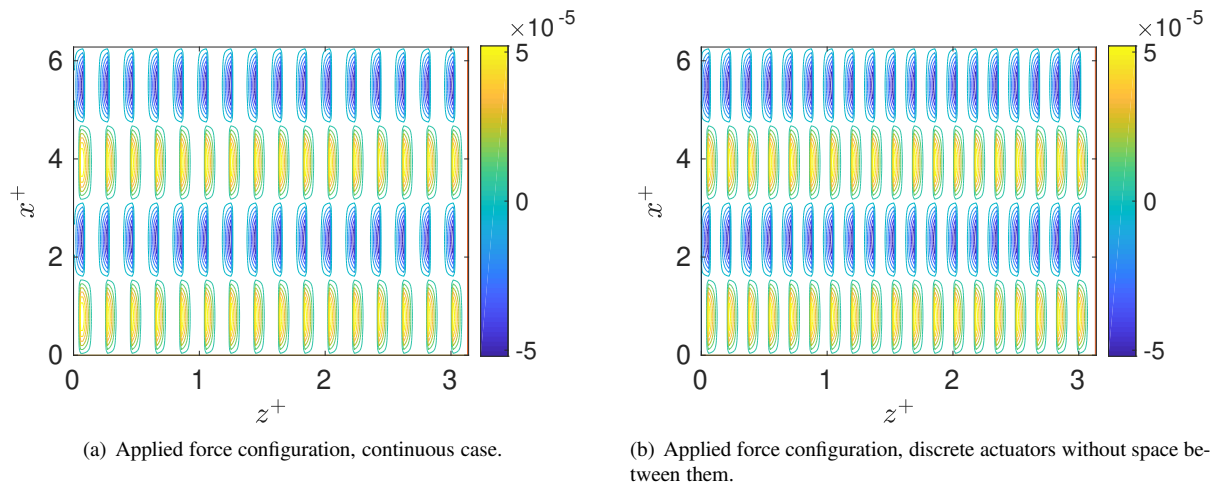

(a) Applied force configuration, continuous case.

(b) Applied force configuration, discrete actuators without space between them.

Figure 4: DNS study. Spatially osillated plasma force, F_z.

4. Results and discussion

Figures 5(a), 5(b) show the Reynolds shear stresses for the force cases, which are compared with the no-force case. A drag reduction of 9% and 4% is observed in Fig.5(a) and 5(b), respectively.
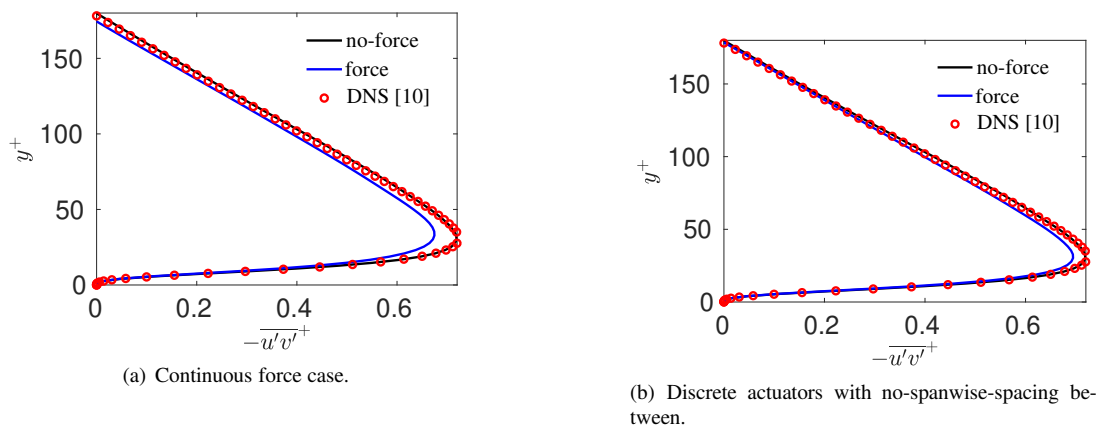

(a) Continuous force case.

(b) Discrete actuators with no-spanwise-spacing between.

Figure 5: Reynolds shear stresses.

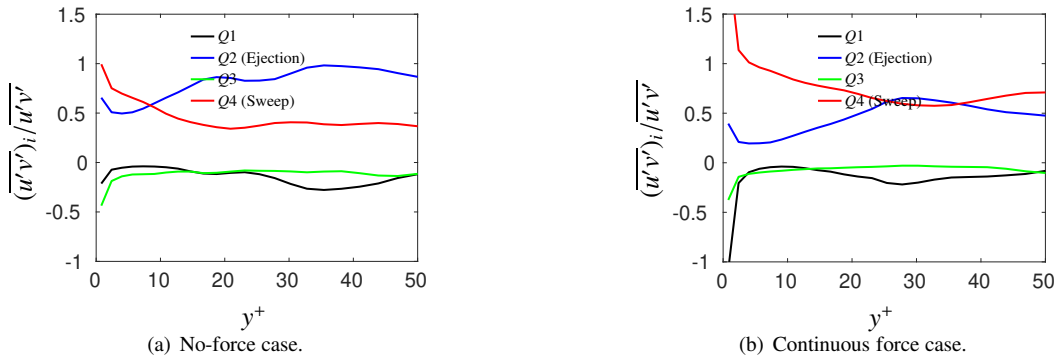(a) No-force case.　　　　　　　　　　　(b) Continuous force case.

Figure 6: Reynolds shear stress from each quadrant normalized by the local mean Reynolds shear stress. Subscript i denotes the quadrant number, Q_i.

A quadrant analysis of the Reynolds shear stresses was made to better compare the flow field structures for the applied force and the no-force cases. To achieve an accurate results, 400 data sets were used for each y^+. Very similar results are obtained in the no-force case (Fig. 6(a)) compared with Kim et al. [9], where they also see dominant sweep events up to a level of $y^+ \approx 10$. In the applied force case, the fourth quadrant events (sweep) dominate over second quadrant events (ejection) up to approximately $y^+ = 25$ and after $y^+ = 38$ (Fig. 6(b)).

5. Conclusions

In this study DBD plasma actuators are applied to a turbulent channel flow to obtain a drag reduction. In order to achieve this, first a single actuator is studied in a stagnant flow, the velocities created are compared with experimental results in the literature. Af ter having a good agreement, DNS study is performed in a fully developed turbulent channel flow. A spanwise oscillated plasma force is applied in the vicinity of the lower wall. The plasma force is created by spanwise aligned multiple DBD plasma actuators. Two different cases have been studied, namely, a continuous force and a force created by discrete plasma actuators without a spanwise spacing. We have achieved a drag reduction of 9% and 4%, respectively. This study is important since a drag reduction is obtained with spanwise oscillated DBD plasma force, that is created by electrodes. Electrodes are light materials which makes them a good candidate in flow control engineering aplications. However we applied a low Reynolds number, $Re_\tau = 180$, this study could be a reference work for the future high Reynolds number studies.

6. Acknowledgments

References

[1] Lionel Agostini and Michael Leschziner. The impact of footprints of large-scale outer structures on the near-wall layer in the presence of drag-reducing spanwise wall motion. *Flow, Turbulence and Combustion*, 100(4):1037–1061, Jun 2018.

[2] A Altıntaş, L Davidson, and SH Peng. A new approximation to modulation-effect analysis based on empirical mode decomposition. *Physics of Fluids*, 31(2):025117, 2019.

[3] Atilla Altıntaş and Lars Davidson. Direct numerical simulation analysis of spanwise oscillating lorentz force in turbulent channel flow at low reynolds number. *Acta Mechanica*, 228(4):1269–1286, 2017.

[4] N Benard, M Caron, and E Moreau. Evaluation of the time-resolved ehd force produced by a plasma actuator by particle image velocimetry-a parametric study. In *Journal of Physics: Conference Series*, volume 646, page 012055. IOP Publishing, 2015.

[5] T. W. Berger, J. Kim, and C. Lee. Turbulent boundary layer control utilizing the Lorentz force. *Phys. Fluids*, 12:631–649, 2000.

[6] L. Davidson and S. H. Peng. Hybrid LES-RANS: A one-equation SGS model combined with a $k - \omega$ model for predicting recirculating flows. *Int. J. Numer. Fluids*, 43:1003–1018, 2001.

[7] Y. Du and G. E. Karniadakis. Suppressing wall turbulence by means of a transverse traveling wave. *Science*, 288:1230–1234, 2000.

[8] Y. Du, V. Symeonidis, and G. E. Karniadakis. Drag reduction in wall-bounded turbulence via a transverse travelling wave. *J. Fluid Mech.*, 457:1–34, 2002.

[9] J. Kim, P. Moin, and R. Moser. Turbulence statistics in fully developed channel flow at low Reynolds number. *J. Fluid Mech.*, 177:133–166, 1987.

[10] R. D. Moser, J. Kim, and N. N. Mansour. DNS of turbulent channel flow up to Re_τ=590. *Phys. Fluids*, 11:943–945, 1999.

[11] W Shyy, B Jayaraman, and A Andersson. Modeling of glow discharge-induced fluid dynamics. *Journal of applied physics*, 92(11):6434–6443, 2002.